Supporting information

Effect of polymerization of zwitterionic monomers on their intrinsic antifreeze activity

Shuya Tanaka,[a] Masanori Nagao,*[a] Hayato Yoshitake,[a] Hikaru Matsumoto,[a] Yuji Higuchi,[b] and Yoshiko Miura*[a]

[a]Department of Chemical Engineering, Kyushu University, 744 Motooka, Nishi-ku, Fukuoka 819-0395, Japan.
[b]Research Institute for Information Technology, Kyushu University, 744 Motooka, Nishi-ku, Fukuoka 819-0395, Japan.

E-mail: miuray@chem-eng.kyushu-u.ac.jp
E-mail: nagaom@chem-eng.kyushu-u.ac.jp

Table of Contents

1. Materials and Methods

Acryloyl chloride (stabilized with Phenothiazine) (> 90%), *S*-2,3-diaminopropanoic acid hydrochloride (> 98%), *N*,*N*-dimethylacrylamide (DMA, 99%), methacryloyl chloride (> 90.0%), propionyl chloride (99%), 8-quinolinol, L-serine (> 99%), and L-sodium ascorbate (AscNa) (98%) were purchased from Tokyo Chemical Industry (Tokyo, Japan). Copper(II) carbonate basic, ethanol, L-lysine monohydrochloride (> 99%), L-ornithine monohydrochloride (> 99%), triethylamine (TEA), and phosphate-buffered saline (PBS, 10 mM of phosphate) were purchased from Fujifilm Wako Pure Chemical Industries (Tokyo, Japan). EosinY disodium salt (> 85%) and Triton X-100 was purchased from Sigma Aldrich (St. Louis, USA). Preserved blood from sheep was purchased from Cosmo Bio Co., LTD (Tokyo, Japan). AHD solution was prepared by mixing Milli-Q water (10 mL), Triton X-100 (250 mL), and NaOH (40 mg). Sodium 2-(((butylthio)carbonothioyl)thio)propanoate (NaBTPA) was synthesized in our laboratory.[1]

Proton nuclear resonance (^{1}H NMR) spectra were recorded on a JEOL-ECP400 spectrometer (JEOL, Tokyo, Japan) using D_2O as a solvent. Size exclusion chromatography (SEC) analysis was performed on a SEC system equipped with a JASCO DG-980-50 degasser, a JASCO PU-980 pump (JASCO Co., Tokyo, Japan), Shodex OH pak SB-G guard column, and a JASCO RI-2031 Plus RI detector. The analyses were performed at a flow rate of 0.5 $mL \cdot min^{-1}$ by injecting 20 μL of a polymer solution (3 $g \cdot L^{-1}$) in 100 mM $NaNO_3$ aqueous solution (20 °C). All the samples were previously filtered through a 0.22 μm filter. The SEC systems were calibrated using a poly(ethylene oxide) standard. In a hemolysis test, absorbance of the each well at 576 nm was measured with a spectral scanning multimode reader (Thermo).

2. Synthesis of zwitterionic monomers

2.1. Synthetic procedure for L-serine methacrylate (SerMA)

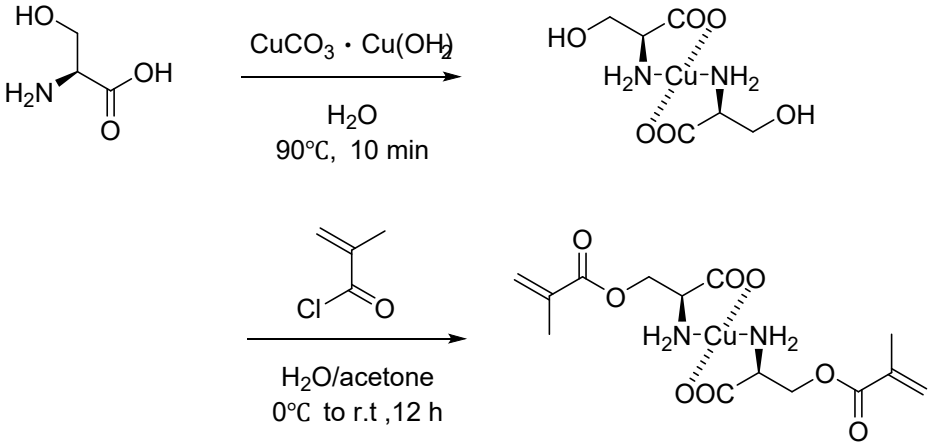

L-Serine (5.0 g, 47.6 mmol, 1.0 eq) and copper carbonate (5.8 g, 26.2 mmol, 0.6 eq) were dissolved in H_2O (50 mL) and stirred at 90 °C for 10 min. After filtration to remove the insoluble residue, acetone (10 mL) and 2 M KOH (27.1 mL) were added to the filtrate. Methacryloyl chloride (5.76 mL, 59.5 mmol, 1.25 eq) in acetone (10 mL) was added dropwise over 20 min at 0 °C. The mixture was then stirred at room temperature for 12 h. The resulting SerMA–copper complex was collected by vacuum filtration and washed sequentially with H_2O, MeOH, and diethyl ether (2.62 g).

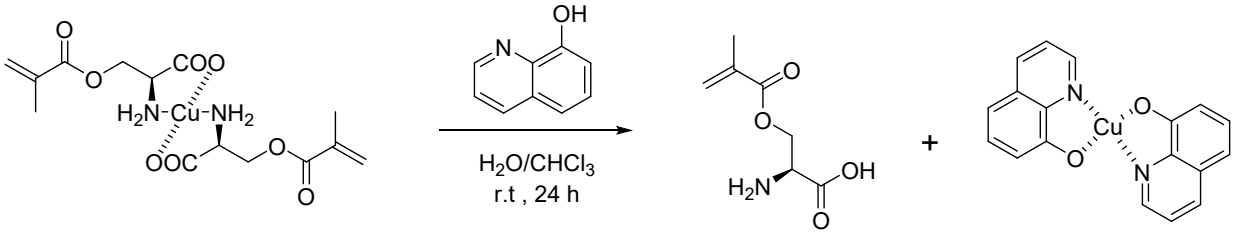

A suspension of SerMA–copper complex (2.62 g, 6.4 mmol, 1.0 eq) and 8-quinolinol (1.1 g, 7.7 mmol, 1.2 eq) in chloroform (10 mL) and H_2O (10 mL) was stirred for 24 h. After filtration to remove the quinolinol–copper complex, the filtrate was concentrated under reduced pressure and recrystallized from THF (150 mL). The resulting white solid was dried under vacuum for 12 h. Subsequently, H_2O (10 mL) was added and the aqueous phase was extracted three times with CH_2Cl_2 (10 mL each). The combined aqueous phase was concentrated under reduced pressure and freeze-dried (400 mg, 36%).

^{1}H NMR (400 MHz, D_2O) δ in ppm: 6.03 (s, *cis* C*H*$_2$=C(CH$_3$), 1H), 5.62 (s, *trans* C*H*$_2$=C(CH$_3$), 1H), 4.44 (d, *J* = 3.6 H, 2H), 3.99 (t, *J* = 3.6 Hz, 1H), 1.78 (s, CH$_2$=C(C*H*$_3$), 3H).

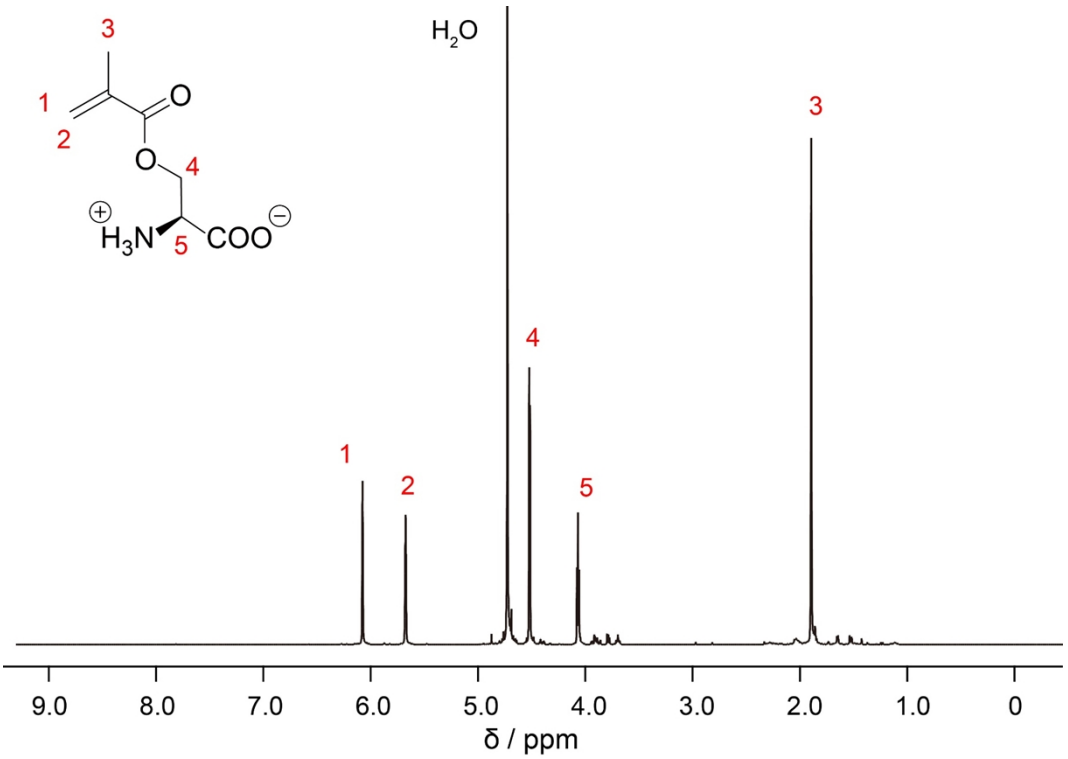

Figure S1. ^{1}H NMR spectrum of L-serine methacrylate (400 MHz, D_2O).

2.2. Synthetic procedure for L-serine acrylate (SerAc)

Acryloyl chloride was used in place of methacryloyl chloride, and the synthesis was carried out under identical conditions to those used for the preparation of SerMA.

^{1}H NMR (400 MHz, D_2O) δ in ppm: 6.28 (dd, *trans* CH_2=CH, J = 1.2 and 17.6 Hz, 1H), 6.02 (dd, CH_2=C*H*, J = 10.8 and 17.6 Hz, 1H), 5.82 (dd, *cis* CH_2=CH, J = 1.2 and 10.8 Hz, 1H), 4.44 (d, J = 4.0 Hz, 2H), 3.92 (t, J = 4.0 Hz, 1H).

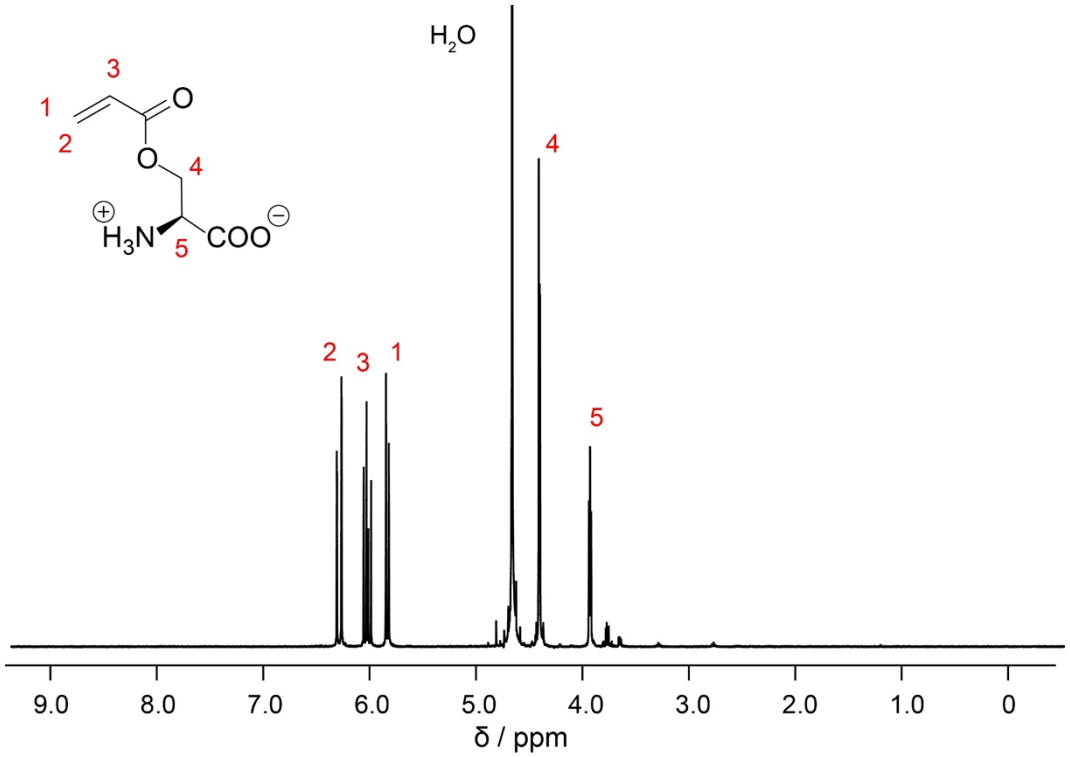

Figure S2. ^{1}H NMR spectrum of L-serine acrylate (400 MHz, D_2O).

2.3. Synthetic procedure for L-2,3-diaminopropanoic acid acrylamide (ApaAm)

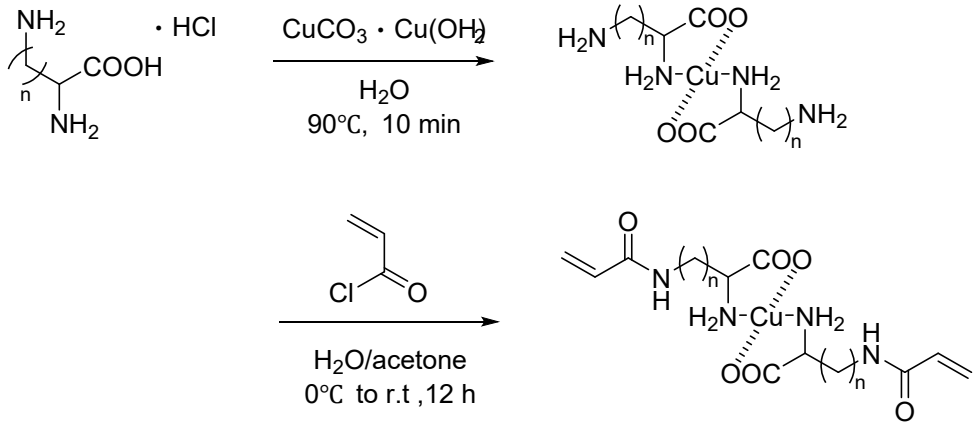

S-2,3-diaminopropanoic acid hydrochloride (4.2 g, 30 mmol, 1.0 eq) and copper carbonate (3.6 g, 16.2 mmol, 0.5 eq) were dissolved in H_2O (50 mL) and stirred at 90 °C for 10 min. After filtration to remove the insoluble residue, acetone (10 mL) and 2 M KOH (27 mL) were added to the filtrate. Acryloyl chloride (3 mL, 37.3 mmol, 2.3 eq) in acetone (10 mL) was added dropwise over 20 min at 0 °C. The mixture was then stirred at room temperature for 12 h. The resulting monomer–copper complex was collected by vacuum filtration and washed sequentially with H_2O, MeOH, and diethyl ether.

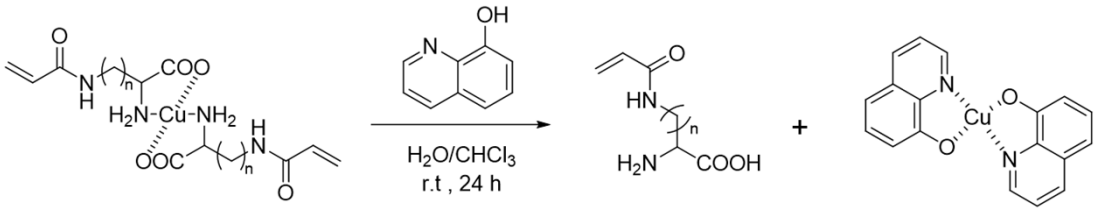

A suspension of monomer–copper complex (2.8 g, 7.5 mmol, 1.0 eq) and 8-quinolinol (1.3 g, 8.9 mmol, 1.2 eq) in chloroform (10 mL) and H_2O (10 mL) was stirred for 24 h. After filtration to remove the quinolinol–copper complex, the filtrate was concentrated under reduced pressure and recrystallized from THF (150 mL). The resulting white solid was dried under vacuum for 12 h. Subsequently, H_2O (10 mL) was added and the aqueous phase was extracted three times with CH_2Cl_2 (10 mL each). The combined aqueous phase was concentrated under reduced pressure and freeze-dried.

^{1}H NMR (400 MHz, D_2O) δ in ppm: 6.12 (dd, CH_2=C*H*, *J* = 9.6 and 16.8 Hz, 1H), 6.06 (dd, *trans* CH_2=CH, *J* = 2.0 and 16.8 Hz, 1H), 5.63 (dd, *cis* CH_2=CH, *J* = 2.0 and 9.6 Hz, 1H), 3.78 (dd, *J* = 3.6 and 6.8 Hz, 1H), 3.68 (d, *J* = 3.6 and 14.8 Hz, 1H), 3.51 (dd, *J* = 6.8 and 14.8 Hz, 1H).

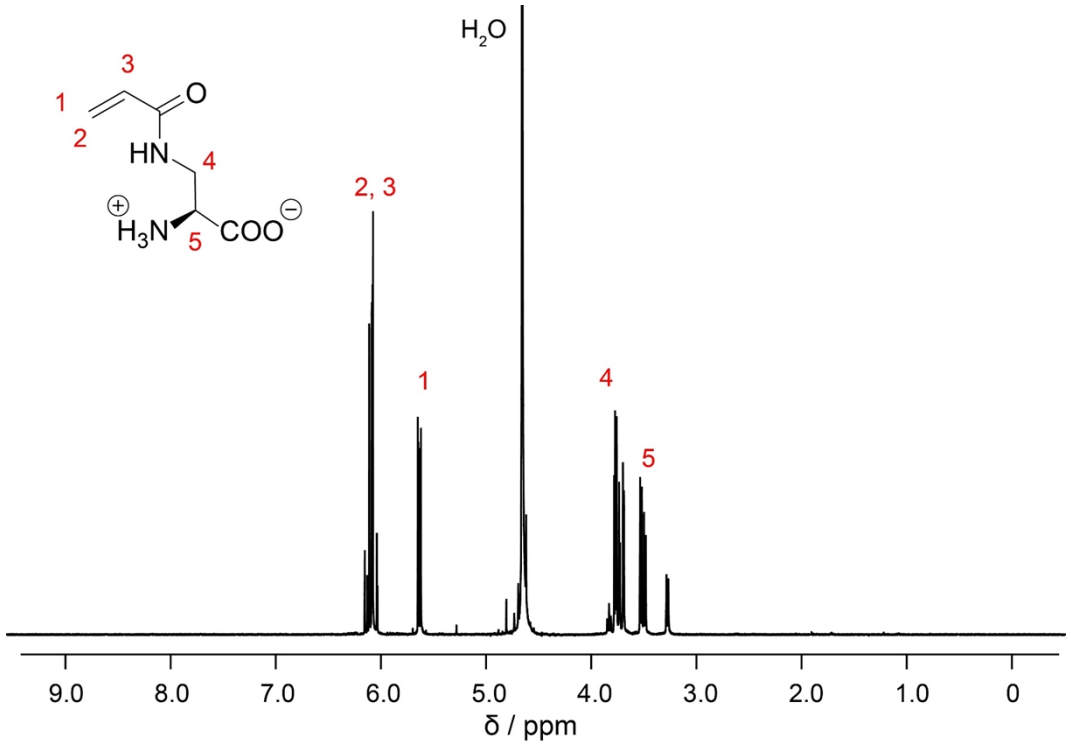

Figure S3. ^{1}H NMR spectrum of L-2,3-diaminopropanoic acid acrylamide (400 MHz, D_2O).

2.4. Synthetic procedure for L-ornithine acrylamide (OrnAAm)

L-Ornithine hydrochloride was used in place of diaminopropanoic acid hydrochloride, and the synthesis was carried out under identical conditions to those used for the preparation of ApaAAm.

^{1}H NMR (400 MHz, D_2O) δ in ppm: 6.12 (dd, CH_2=C*H*, *J* = 9.6 and 16.8 Hz, 1H), 6.06 (dd, *trans* C*H*$_2$=CH, *J* = 2.0 and 16.8 Hz, 1H), 5.63 (dd, *cis* C*H*$_2$=CH, *J* = 2.0 and 9.6 Hz, 1H), 3.60 (t, *J* = 6.0 Hz, 1H), 3.16 (td, *J* = 2.4 and 6.8 Hz, 2H), 1.72 (m, 2H), 1.48 (m, 2H).

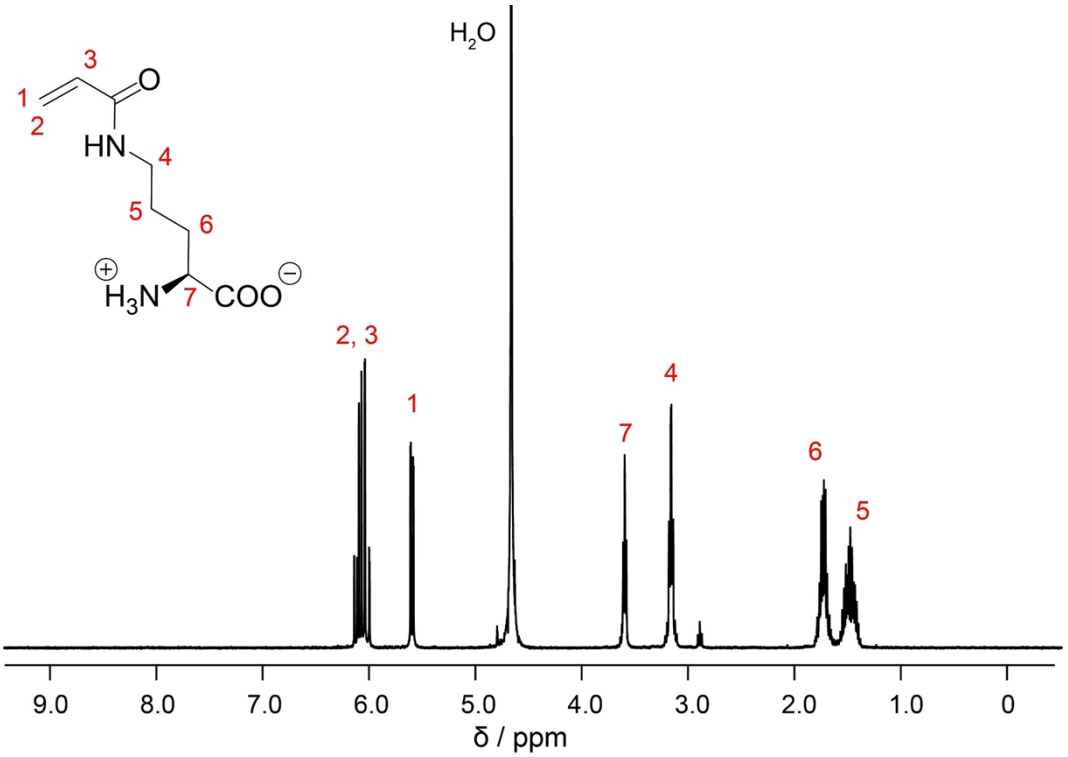

Figure S4. ^{1}H NMR spectrum of L-ornithine acrylamide (400 MHz, D_2O).

2.4. Synthetic procedure for L-propionyl serine

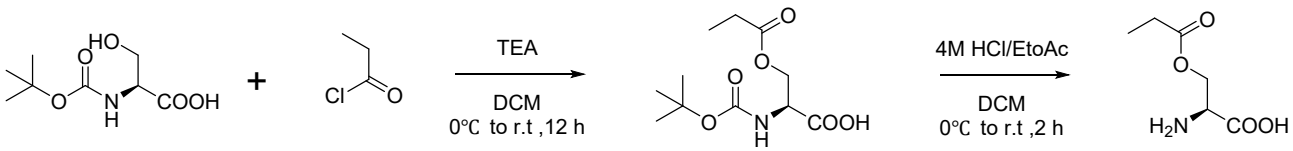

N-Boc-L-Serine (1.00 g, 4.85 mmol, 1 eq) and TEA (1.49 mL, 10.7 mmol, 2.2 eq) were dissolved in DCM (10 mL). Propionyl chloride (510 µL, 5.82 mmol, 1.2 eq) diluted in DCM (5 mL) was added dropwise at 0 °C. The reaction mixture was stirred at room temperature for 12 h. After completion, the mixture was washed sequentially with 0.3 M HCl (×2), Milli-Q water (×1), and saturated NaCl(aq) (×1). While cooling in an ice bath, 4 M HCl in EtOAc was added dropwise. The mixture was stirred at room temperature for 2 h. The resulting white precipitate was collected by vacuum filtration and dried under reduced pressure for 3 h (100 mg, 13%).

^{1}H NMR (400 MHz, D_2O) δ in ppm: 4.45 (dd, *J* = 4.8 and 12.4 Hz, 1H), 4.36 (dd, *J* = 2.8 and 12.4 Hz, 1H), 4.18 (t, *J* = 4.0 Hz, 1H), 2.27 (q, *J* = 7.6 Hz, 2H), 0.93 (t, *J* = 7.6 Hz, 3H).

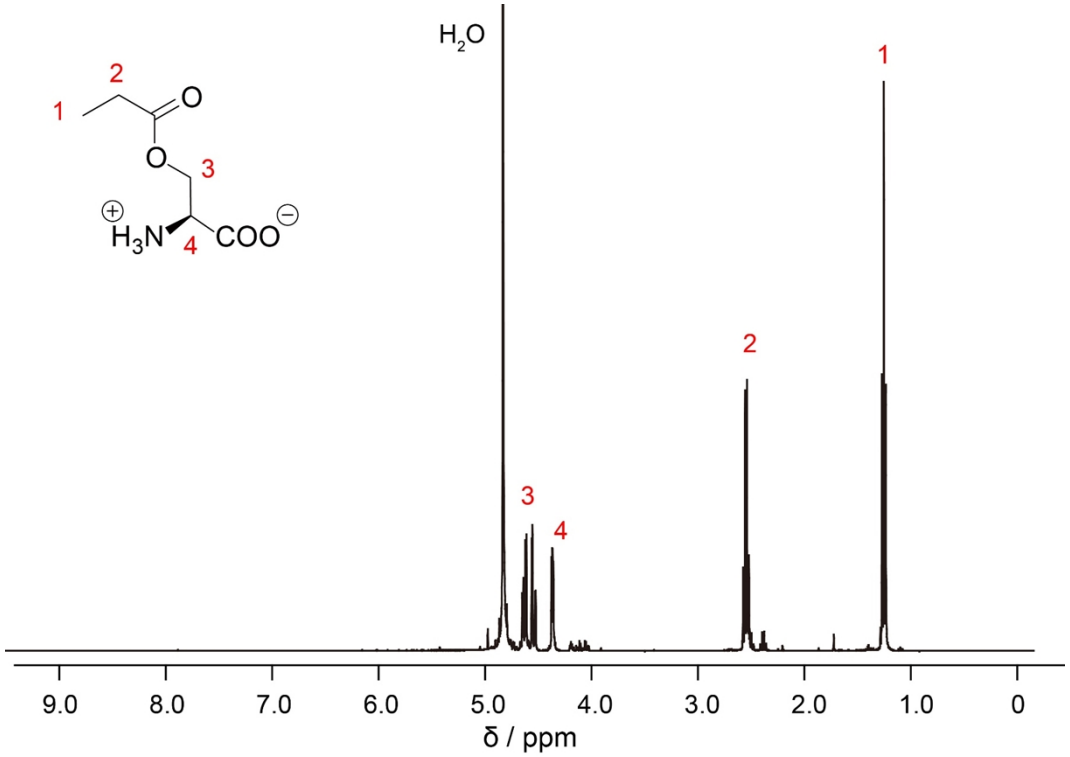

Figure S5. ^{1}H NMR spectrum of L-propionyl serine (400 MHz, D_2O).

3. Preparation of zwitterionic polymers

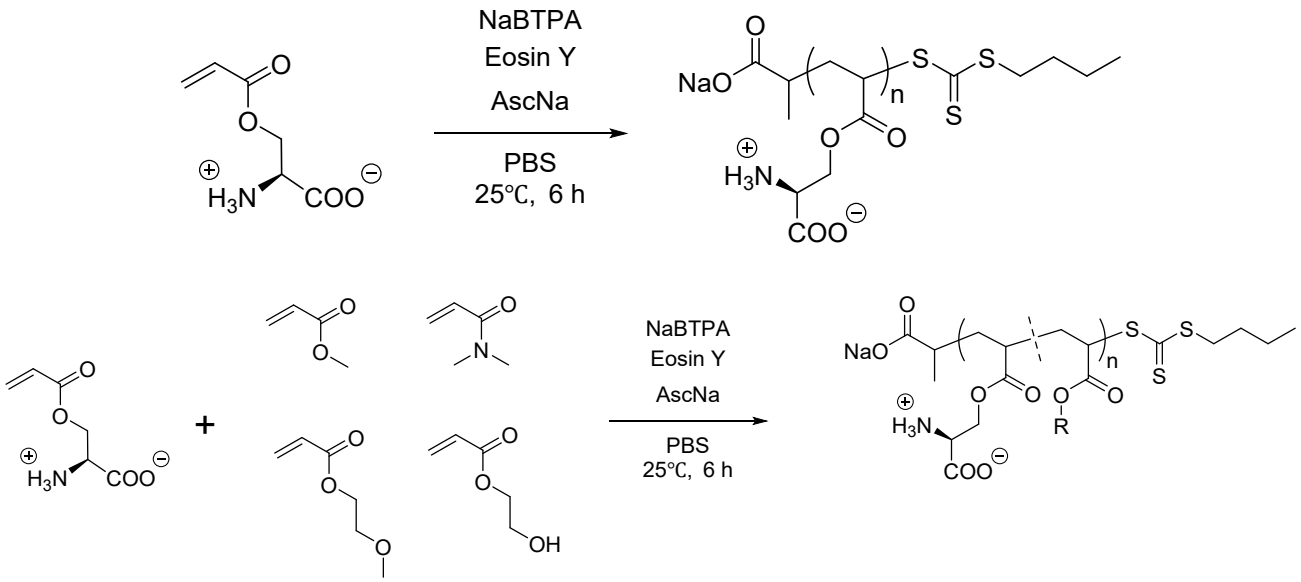

Monomers, NaBTPA (RAFT agent), sodium ascorbate, and Eosin Y (catalyst) were dissolved in PBS. The monomer concentration and the ratio of reactants are shown in Table S1. The molar ratio of [RAFT]:[L·Asc·Na]:[Eosin Y] was 1:0.01:1. The reaction was carried out under green light irradiation (LED, 527 nm) at 25°C for 6 h. The monomer conversion was determined by ^{1}H NMR (D_2O). The polymer solution was vacuum-dried and subsequently dissolved in Milli-Q water. The solution was then added to an ultrafiltration filter (MWCO: 3000) and purified by centrifugation (14,000 × g, 15 min, three times). Following purification, the tip of the filter was inverted, and the sample was recovered by centrifugation again (1,000 × g, 5 min). The samples collected were then lyophilized.

Table S1. Results of PET-RAFT polymerization for poly(SerAc)

Polymer	SerAc	NaBTPA	Eosin Y	L‧Asc‧Na	[Monomer]	Conversion	M_n	M_w	$Đ$	DP from NMR
	mg (mmol)	mg (μmol)	μg (μmol)	mg (μmol)	(mol/L)	(%)	(g/mol)	(g/mol)		
$SerAc_{20}$	32 (0.2)	2.6 (10)	69.2 (0.1)	2.0 (10)	0.5	71	900	1,000	1.14	20
$SerAc_{85}$	32 (0.2)	0.52 (2.0)	13.8 (0.02)	0.40 (2.0)	0.5	85	3,200	4,600	1.46	85
$SerAc_{128}$	32 (0.2)	0.35 (1.3)	9.2 (0.013)	0.26 (1.3)	0.5	79	3,900	5,900	1.51	128

Table S2. Results of PET-RAFT copolymerization of SerAc with nonionic monomers

Polymer	SerAc	Nonionic monomer	NaBTPA	Eosin Y	L‧Asc‧Na	[Monomer]	Conversion	M_n	M_w	$Đ$	DP from NMR	
	mg (mmol)	mg (mmol)	mg (μmol)	μg (μmol)	mg (μmol)	(mol/L)	(%)	(g/mol)	(g/mol)		SerAc	Nonionic monomer
$SerAc_{29}MA_{11}$	16 (0.1)	9 (0.1)	1.0 (4.0)	27.7 (0.04)	0.79 (4.0)	0.5	81	1800	2,300	1.26	29	11
$SerAc_{25}MEA_{27}$	16 (0.1)	13 (0.1)	1.0 (4.0)	27.7 (0.04)	0.79 (4.0)	0.5	83	2000	2,900	1.44	25	27
$SerAc_{28}HEA_{37}$	16 (0.1)	12 (0.1)	1.0 (4.0)	27.7 (0.04)	0.79 (4.0)	0.5	88	2,000	2,700	1.33	28	37
$SerAc_{26}DMA_{24}$	16 (0.1)	10 (0.1)	1.0 (4.0)	27.7 (0.04)	0.79 (4.0)	0.5	76	1,600	2,300	1.43	26	26

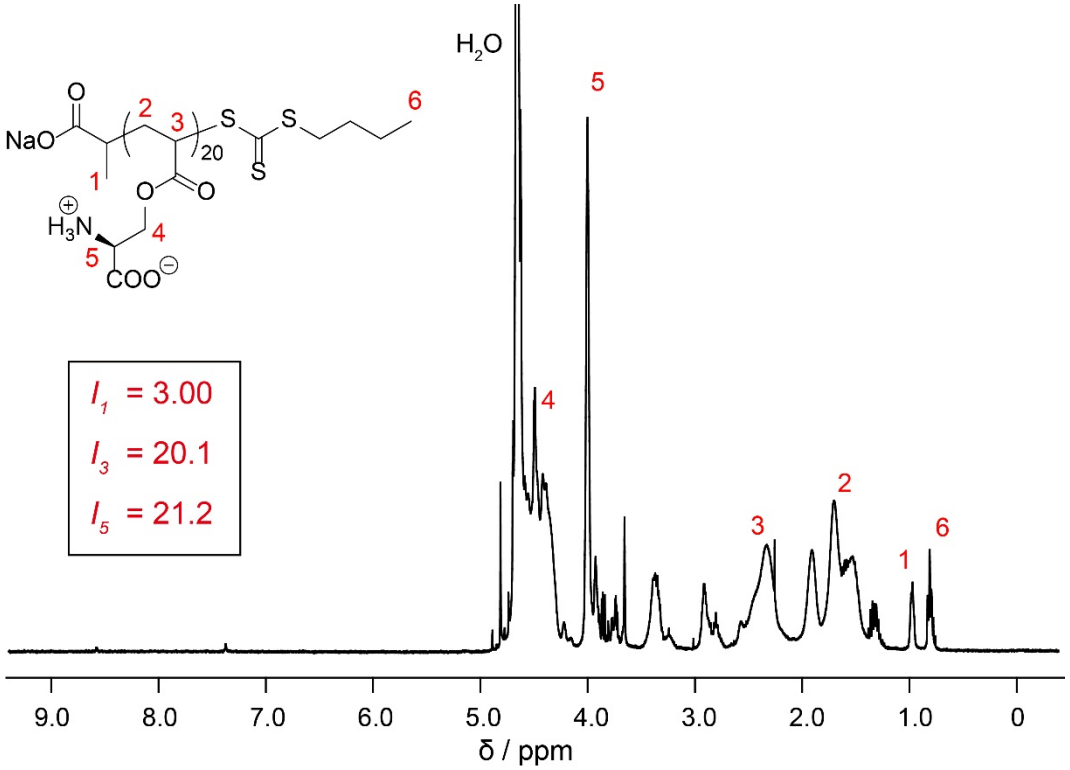

Figure S6. ^{1}H NMR spectrum of polySerAc$_{20}$ (400 MHz, D_2O).

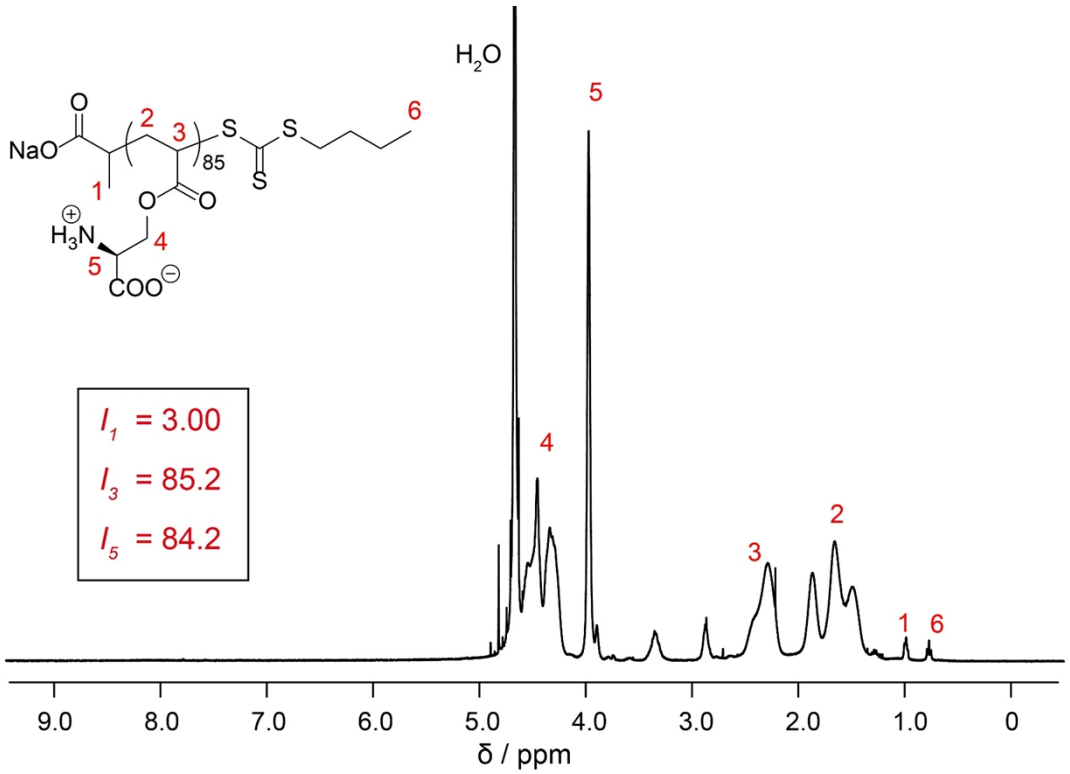

Figure S7. ^{1}H NMR spectrum of polySerAc$_{85}$ (400 MHz, D_2O).

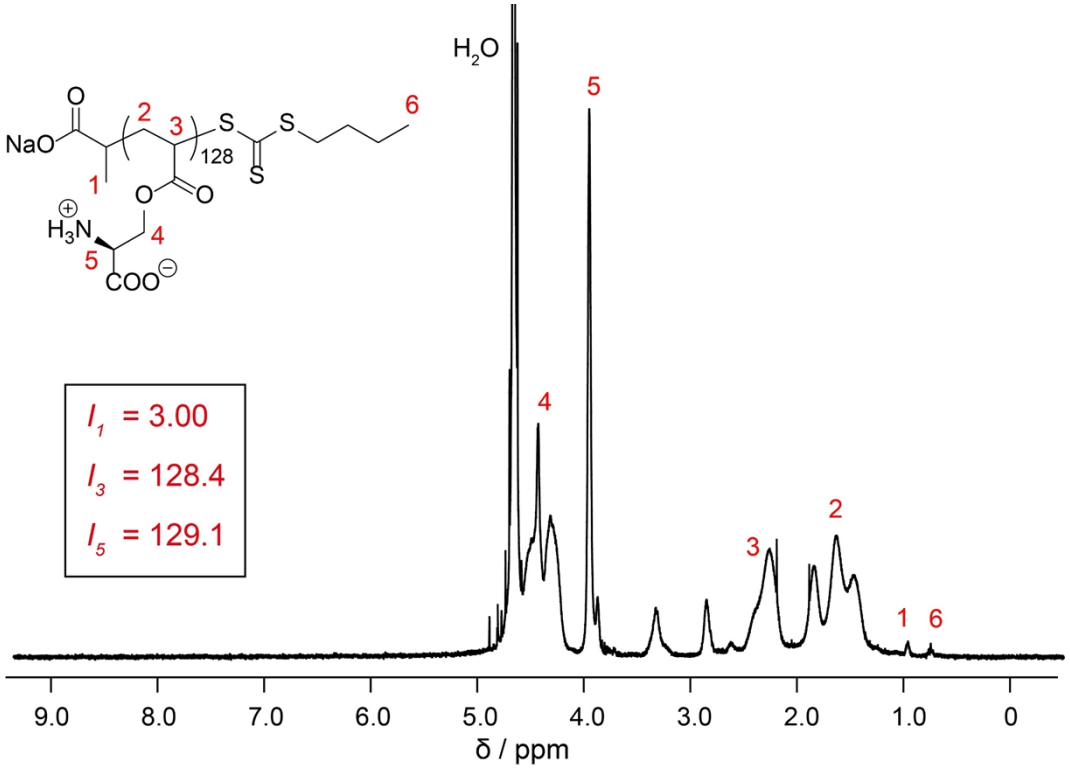

Figure S8. ^{1}H NMR spectrum of polySerAc$_{128}$ (400 MHz, D_2O).

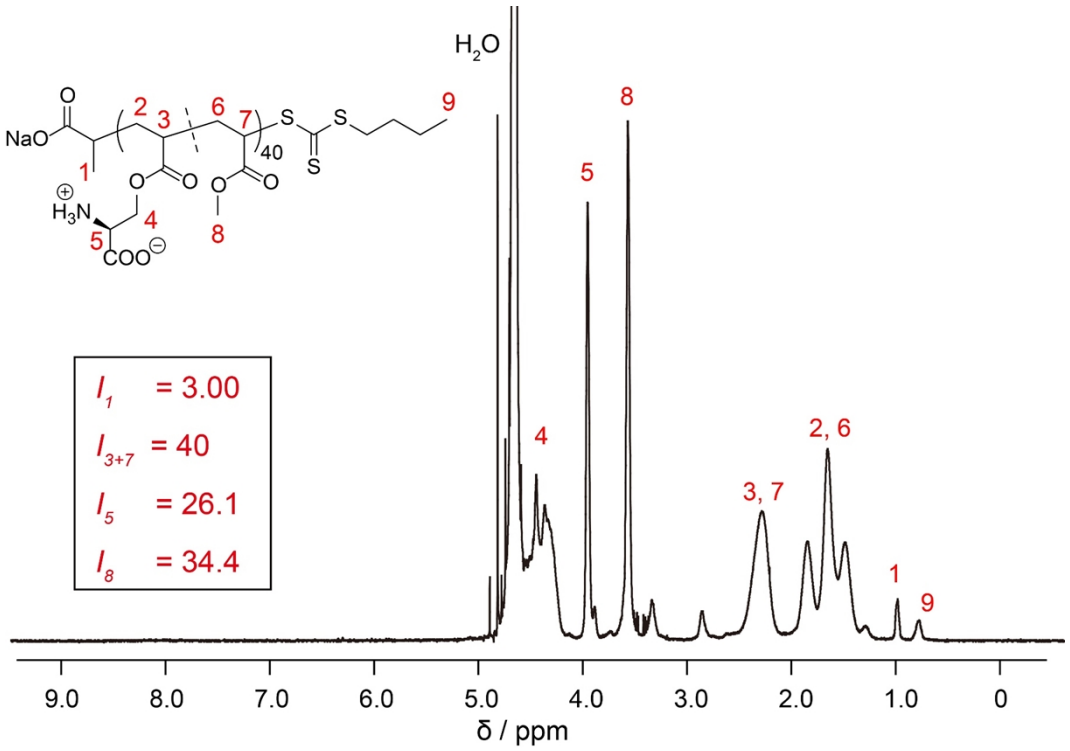

Figure S9. ^{1}H NMR spectrum of poly(SerAc$_{29}$-*st*-MA$_{11}$) (400 MHz, D_2O).

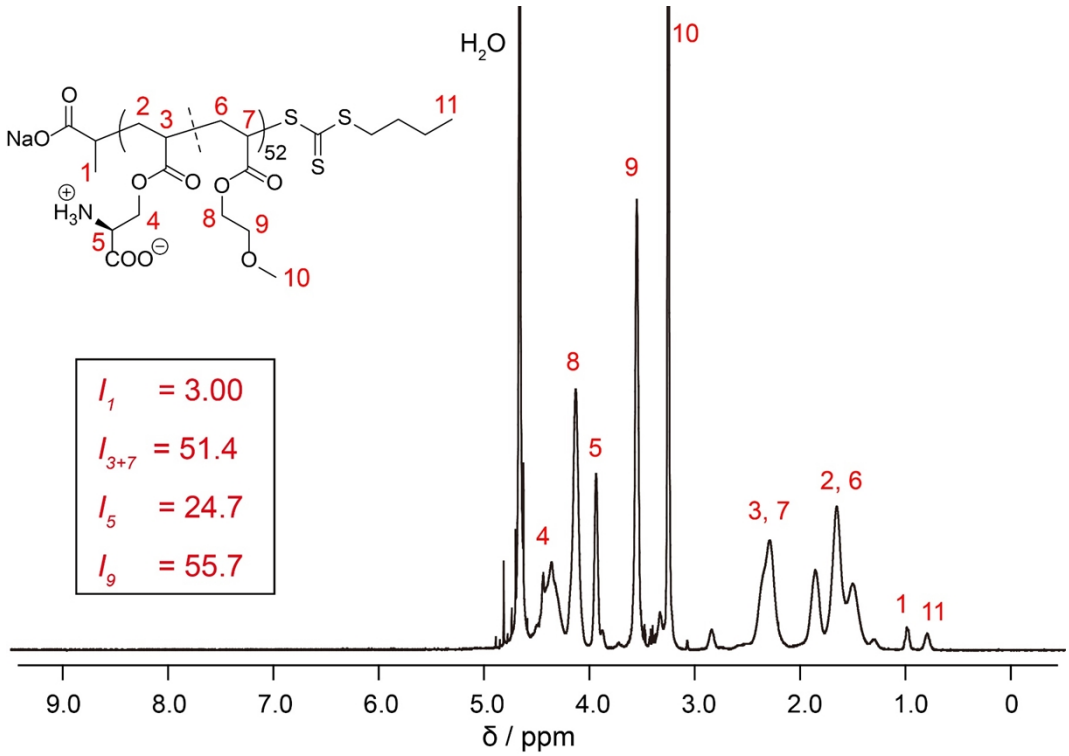

Figure S10. ^{1}H NMR spectrum of poly(SerAc$_{25}$-*st*-MEA$_{27}$) (400 MHz, D_2O).

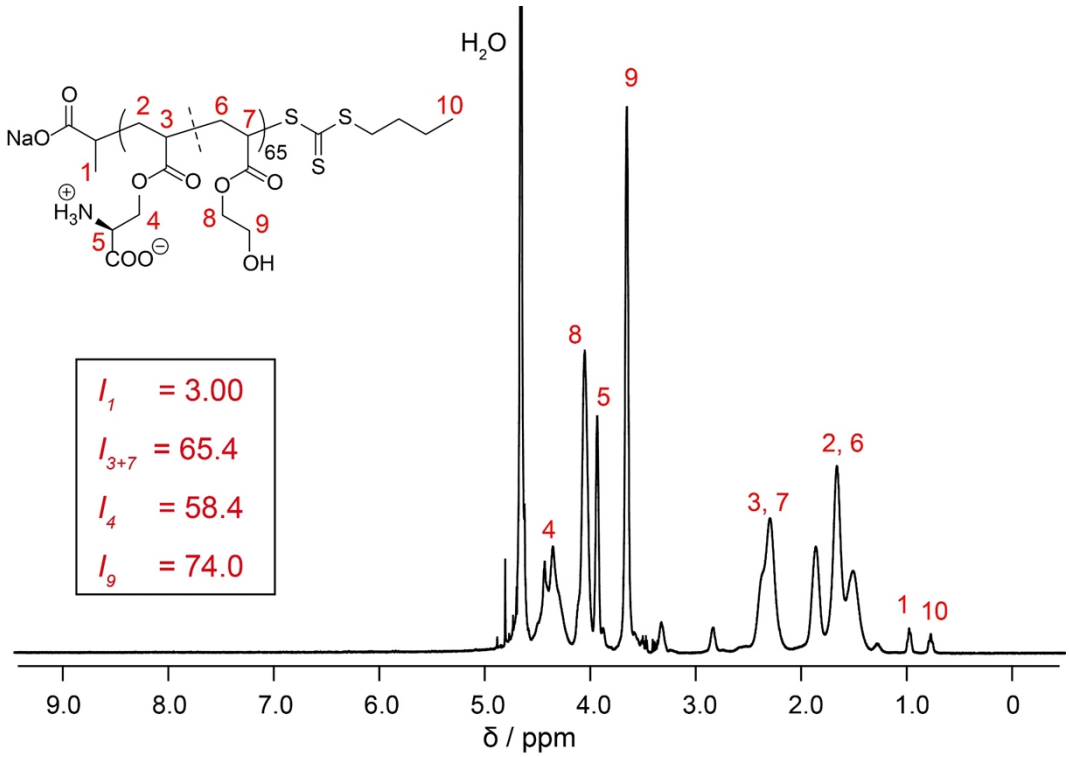

Figure S11. ^{1}H NMR spectrum of poly(SerAc$_{28}$-*st*-HEA$_{37}$) (400 MHz, D_2O).

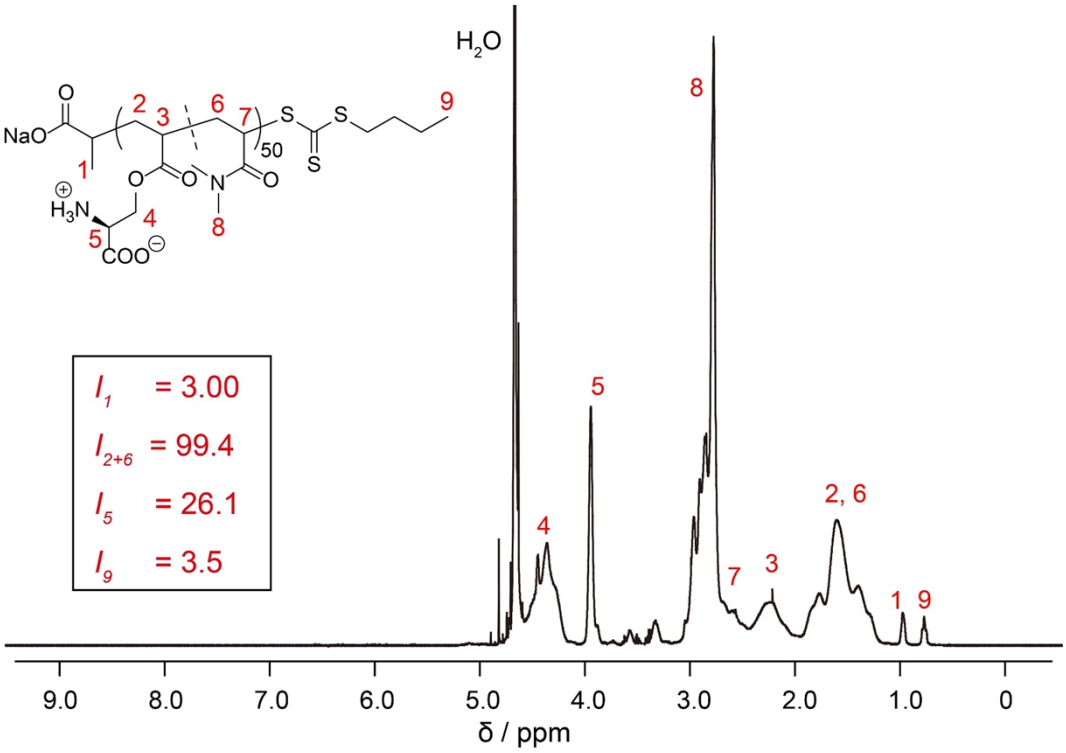

Figure S12. ^{1}H NMR spectrum of poly(SerAc$_{26}$-*st*-DMA$_{24}$) (400 MHz, D_2O).

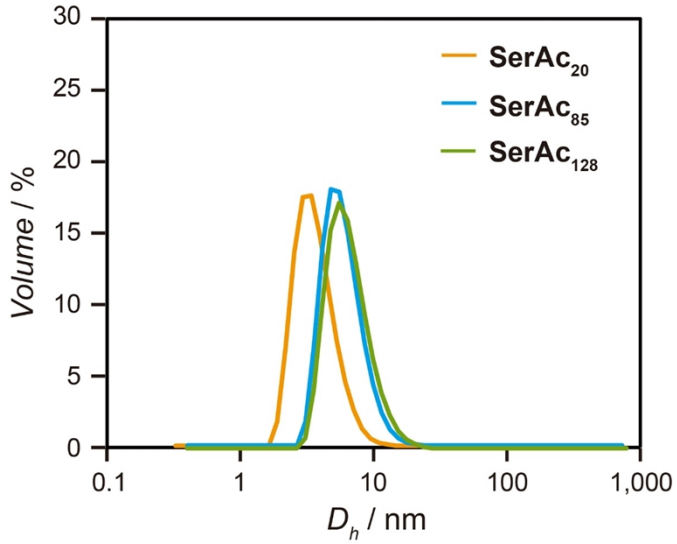

Figure S13. Distribution of D_h of the zwitterionic polymer solution (3 g L^{-1}) measured by DLS in a 10 mM phosphate buffer. The distributions are presented as volume.

4. Ice recrystallization inhibition assay

A 10 μL droplet of polymer in PBS solution was dropped from 1.4 meters onto a glass microscope coverslip, which was placed on top of an aluminium plate cooled to −78 °C using dry ice. The droplet froze instantly upon impact with the plate, spreading out and forming a thin wafer of ice. This wafer was then placed on a cryostage held at −8 °C (Linkam 10021, Tadworth, Surrey, UK). The wafer was then left to anneal for 30 minutes at −8 °C. The ten largest ice crystals in the field of view were measured and the single largest length in any axis recorded (Nikon Eclipse Ts2). This was repeated for at least three wafers, and the average (mean) value was calculated to find the largest grain dimension along any axis. The average of this value from three individual wafers was calculated to give the mean largest grain size (MLGS).

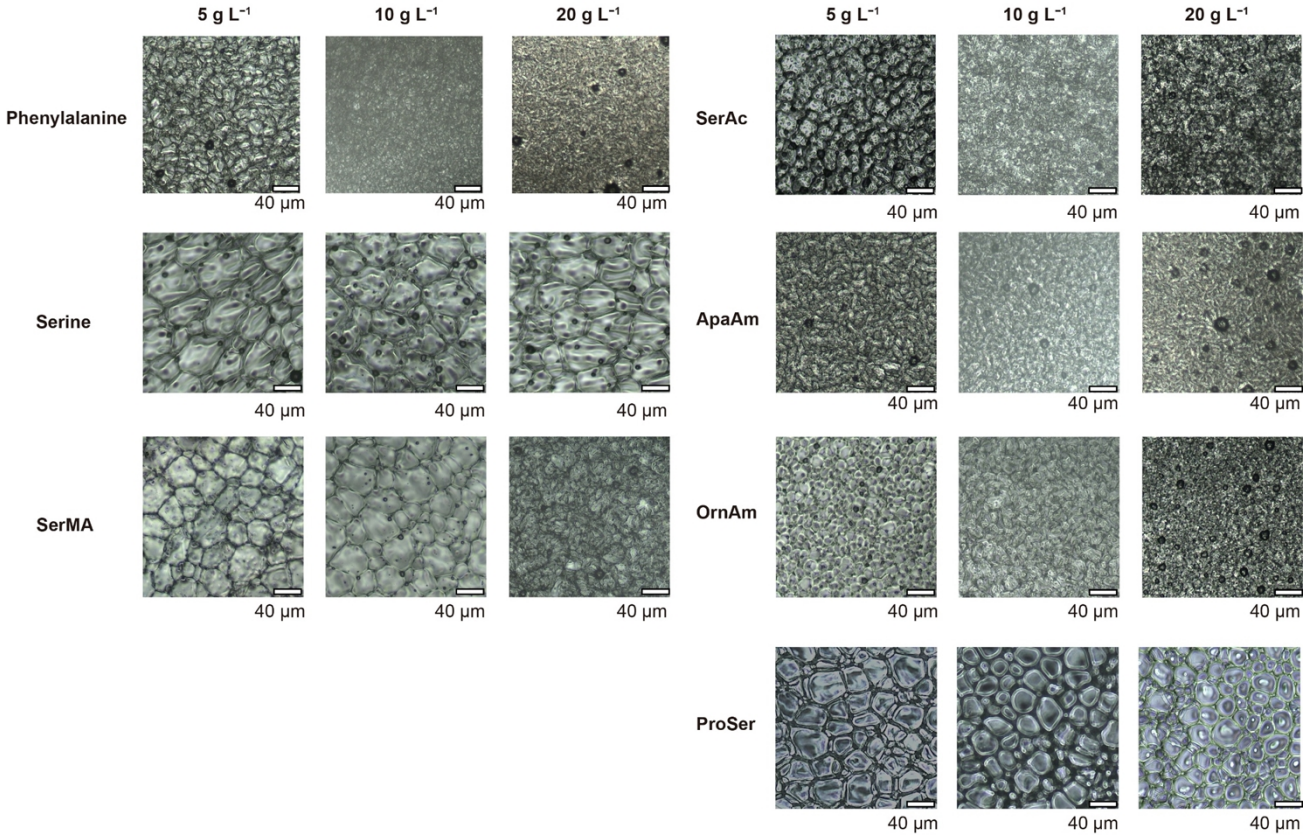

Figure S14. Representative micrographs showing ice crystals grown with each zwitterionic compound.

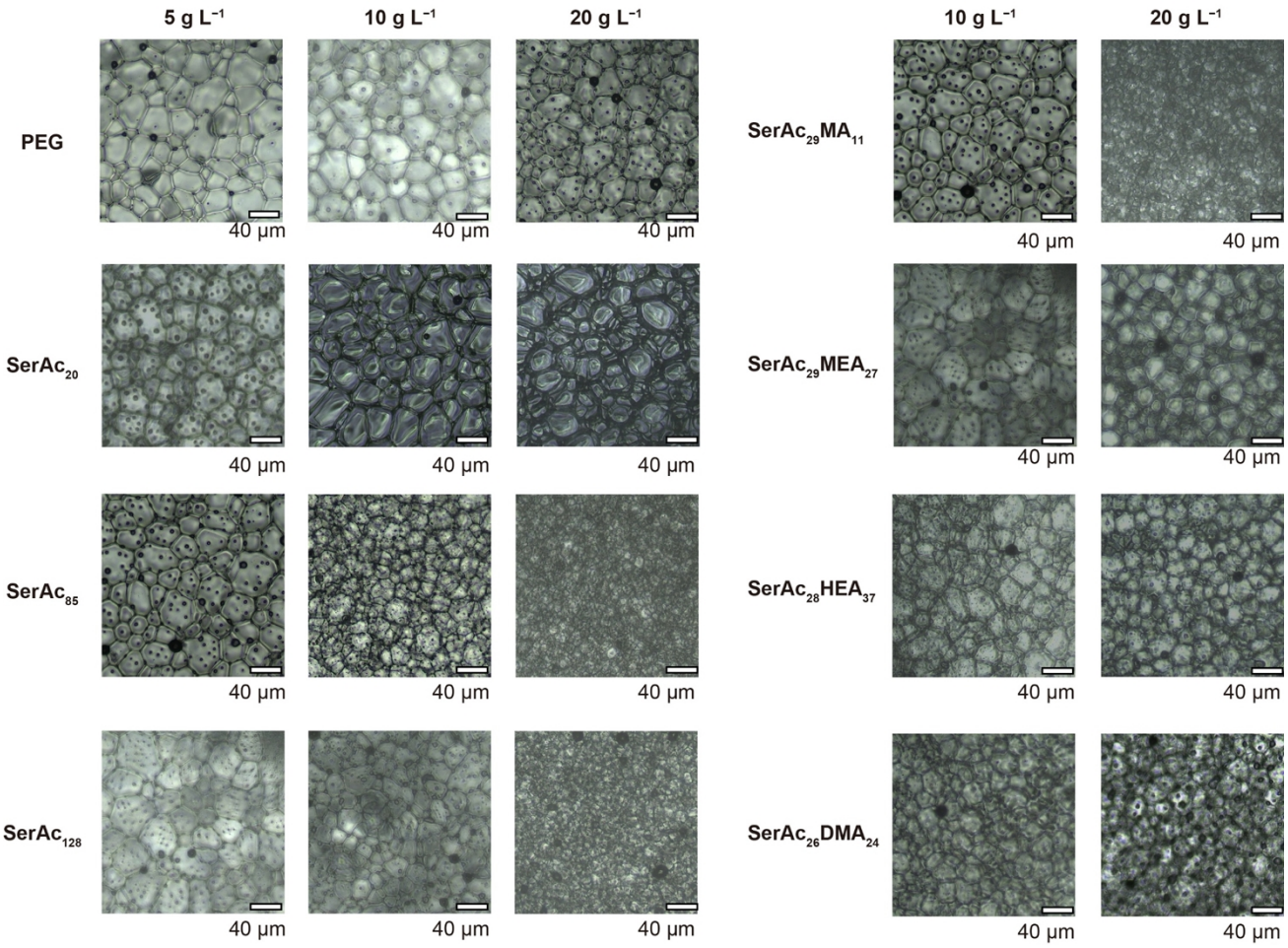

Figure S15. Representative micrographs showing ice crystals grown with each zwitterionic polymer.

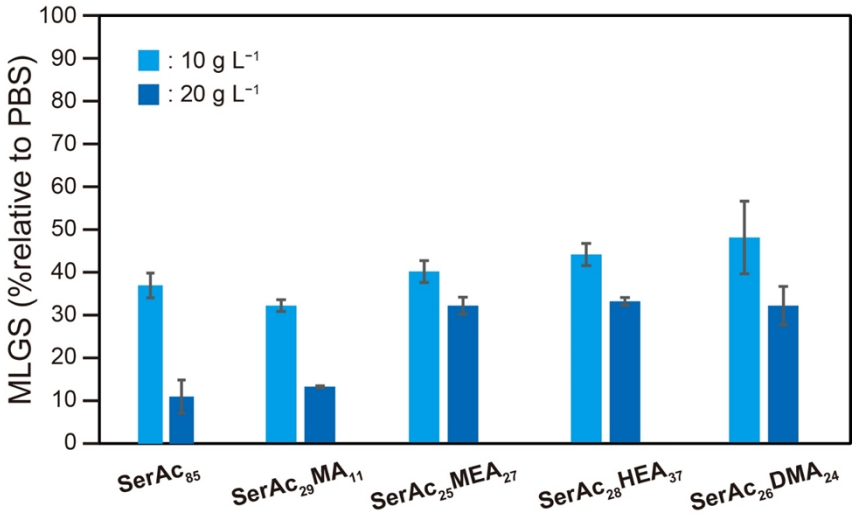

Figure S16. Ice recrystallization inhibition activity of the zwitterionic copolymers evaluated by the splat-cooling assay. Mean largest grain size (MLGS) of each compound relative to a PBS control, expressed as a percentage. Error bars represent the standard deviation from at least three measurements.

5. Cryoprotection experiments using red blood cells

Sheep blood in Alsevers solution (1 mL) was added to a maicrotube and centrifuged at 2000 rpm for 5 min to concentrate the red blood cells (RBCs). The supernatant was removed and replaced with 500 μL of PBS solution. The RBCs were concentrated by centrifugation again. This process was repeated twice. Finally, the blood suspension in PBS was obtained (500 μL). The each following solution (500 μL) was added to cryopreservation vials along with 500 μL of the RBC suspension: a 10 wt% DMSO solution in PBS, a SerAc solution (10 g L^{-1} in PBS), and a $SerAc_{85}$ solution (10 g L^{-1} in PBS). The samples were immersed in liquid nitrogen for 10 min. Afterward, the samples were thawed in a 37°C water bath for 10 min. The samples were transferred from cryovials to microtubes, centrifuged for 5 min, and 20 μL of the supernatant was added to 100 μL of AHD solution. The absorbance at 576 nm was measured using a plate reader. The amount of hemoglobin leakage was used to determine the degree of RBC damage caused by freezing, and the RBC protection efficiency (Recovery value) was calculated using the following equation:

$$\text{Recovery} = 100 \times (\text{Max} - \text{Value})/(\text{Max} - \text{Min})$$

where:

Min = absorbance of RBCs frozen in PBS alone

Max = absorbance of RBCs completely lysed using RBC lysis buffer

Value = absorbance of the tested samples

6. Molecular dynamics simulations

For all-atom molecular dynamics (MD) simulations under three-dimensional periodic boundary conditions, the following systems were investigated in this study: water solutions of phenylalanine, L-serine acrylate, and L-propionyl serine. The concentration of all the solutions was 1 M, and the number of zwitterionic monomers in the solutions was 5. The number of water molecules in the pure water system was 200. The packmol package[2] was used to construct models of solutions and pure water with a density of 1.0 g cm^{-3}. Typical MD simulation snapshots are shown in Fig. S16 to illustrate the simulation setup.

Third-order density-functional tight-binding (DFTB) MD simulations using the opensource DFTB+ software (version 20.1)[3] in an *NpT* ensemble were used along with the parameter sets 3ob[4,5] and 3obw[6]. The H5 correction[7] was applied with the following specifications to precisely model the hydrogen bonds in the solutions: $S_r = 0.68$, $S_w = 0.23$, $k_{OH} = 0.045$, and $k_{NH} = 0.0675$. A previous study[8] confirmed that the radial distribution functions for water molecules are similar in the TIP4P model[9] and in DFTB with 3obw. A time step of 1 fs was used for the integration of the equations of motion using the velocity Verlet algorithm. The temperature was kept constant at 300 K by a Nose−Hoover thermostat[10] with a coupling strength of 3200 cm^{-1}. The pressure was isotropically controlled at 1 atm by a Berendsen barostat[11] with a damping time of 0.1 ps. After the relaxation calculation of 100 ps at least, the production runs were performed over 500 ps to analyze the rotational dynamics and the structure of water molecules around zwitterionic monomers. After the equilibration, the changes in the potential energies and cell volume were monitored during the simulations. Significant changes were not observed in the product runs.

To reveal the water dynamics around zwitterionic monomers, the rotational dynamics of water molecules were evaluated. The time correlation function of the dipole moments of water molecules was analyzed. The angle between the dipole moment of water molecules at time t and that at the initial time for the analysis, $t = 0$, $\theta(t)$, was calculated. The relaxation time of each water molecule, τ, was estimated when the correlation disappeared: $\cos \theta(t) < e^{-1}$. Then, the average relaxation time for all water molecules, $\langle\tau\rangle$, was calculated. The relaxation time of water molecules as a function of the distance from the zwitterionic monomer was also analyzed. The distance is between the atoms in the zwitterionic monomer and the oxygen atoms of water at the initial state for the calculation of the rotational dynamics.

Hydrogen bonds can be defined by the geometric conditions between the water molecules.[12] Referring to the water molecule supplying the H atom as the donor and the water molecule receiving the H atom as the acceptor, the conditions were as follows: (i) the distance between the O atoms of two water molecules is less than 3.60 Å, (ii) the distance between the H atom of the donor and the O atom of the acceptor is less than 2.45 Å, and (iii) the angle between the OH vector of the donor and the OH vector between the donor and acceptor is greater than 150°. Condition (i) is related to the distance, where the separation between the two O atoms is smaller than the first minimum of the radial distribution function. Conditions (ii) and (iii) are related to the orientation between water molecules.

The number of water molecules satisfying condition (i) was referred to as the number of nearest-neighbor molecules, N_{NN}. The number of hydrogen bonds between water molecules, $N_{HB,}$ and the number of nearest-neighbor water molecules, $N_{NN,}$ were counted and used to calculate the normalized parameter N_{HB}/N_{NN}. In addition to the average values of N_{HB}/N_{NN} in the system, N_{HB}/N_{NN} as a function of the distance from the zwitterionic monomer was also analyzed. The distance is between the atoms in the zwitterionic monomer and the oxygen atoms of water.

Table S3 shows $\langle\tau\rangle$ and $\langle N_{HB}/N_{NN}\rangle$ for pure water and zwitterionic solutions. By the addition of zwitterionic monomers, the rotational relaxation of water molecules slows down compared to pure water, while the normalized number of hydrogen bonds between water molecules decreases. Our previous study[13] of the water dynamics around 15 osmolytes showed that zwitterions slow the rotational relaxation of water, with rotational relaxation times of 2.39 ps or higher, and a slowest of 2.79 ps. Molecules that tend to accelerate water dynamics were urea and guanidine, which showed rotational relaxation times of 2.21 ps and 2.19 ps, respectively. The previous study has shown that when the rotational relaxation of water is slow, N_{HB}/N_{NN} increases, whereas when the rotational relaxation of water is fast, N_{HB}/N_{NN} decreases. In the zwitterions, N_{HB}/N_{NN} were over 0.623, with a maximum of 0.650. For urea and guanidine, the values were 0.616 and 0.611, respectively. Considering the results of this simulation and the previous study, the zwitterionic monomers used in this study break the hydrogen bonds between water molecules and accelerate water dynamics.

The influence of the moiety of the zwitterionic monomer on the water molecules was analyzed in detail. Fig. S17 shows the RDF from the O atom of the zwitterion, the average N_{HB}/N_{NN} at each distance, and the average τ at each distance in phenylalanine, L-serine acrylate, and L-propionyl serine. In the RDF, a peak for H atoms is observed, followed by a peak for O atoms, which indicates that the negatively charged O atoms of the zwitterions strongly attract the positively charged H atoms of the water molecules. The N_{HB}/N_{NN} is smaller than that of pure water, shown by the dashed line, up to the second peak of the RDF. This indicates that the hydrogen bonds between water molecules are broken around the O atoms. On the other hand, the τ is larger near the O atoms than the average value. This means that the O atoms strongly bind the water molecules. These results are common to all zwitterions used in this study. The results around the N atom of zwitterions in Fig. S18 show a similar trend.

The results around the end opposite the zwitterionic moiety, which are C atoms in $-C_6H_5$, $-CHCH_2$, and $-CH_2CH_3$, in phenylalanine, L-serine acrylate, and L-propionyl serine, respectively, are shown in Fig. S19. In the RDF, there is no difference in the peak positions of H and O, and the maximum value of the peak is only slightly greater than 1. This is because the carbon atoms are neutral, and the water molecules are not strongly attracted to them. On the other hand, the N_{HB}/N_{NN} and τ values are slightly larger than average. This means that hydrogen bonds are formed between water molecules, restricting their rotation. Although there are slight differences between the three types of zwitterions, they tend not to change significantly. These results reveal that at room temperature, the three types of zwitterions have the effect of breaking the hydrogen bonds between water molecules and accelerating the dynamics of water; however, there are no major differences.

Table S3. The average rotational relaxation time of water molecules, $\langle\tau\rangle$, for each solution and the normalized parameter $\langle N_{HB}/N_{NN}\rangle$, where N_{HB} is the average number of hydrogen bonds between water molecules and N_{NN} is the number of nearest-neighbor water molecules

	$\langle\tau\rangle$ (ps)	$\langle N_{HB}/N_{NN}\rangle$
Pure Water	2.11	0.617
Phenylalanine solution	2.38	0.607
L-serine acrylate solution	2.35	0.601
L-propionyl serine solution	2.34	0.600

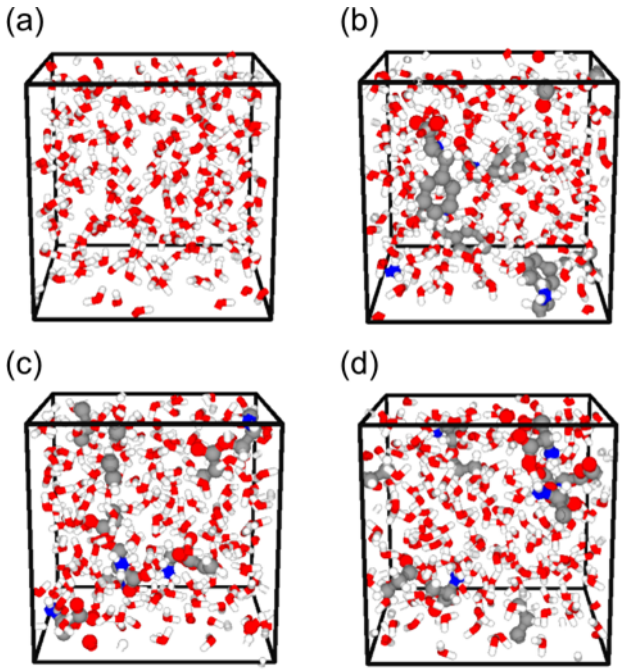

Figure S17. Typical MD simulation snapshots for (a) pure water, (b) phenylalanine, (c) L-serine acrylate, and (d) L-propionyl serine. Red, white, gray, and blue represent oxygen, hydrogen, carbon, and nitrogen atoms, respectively.

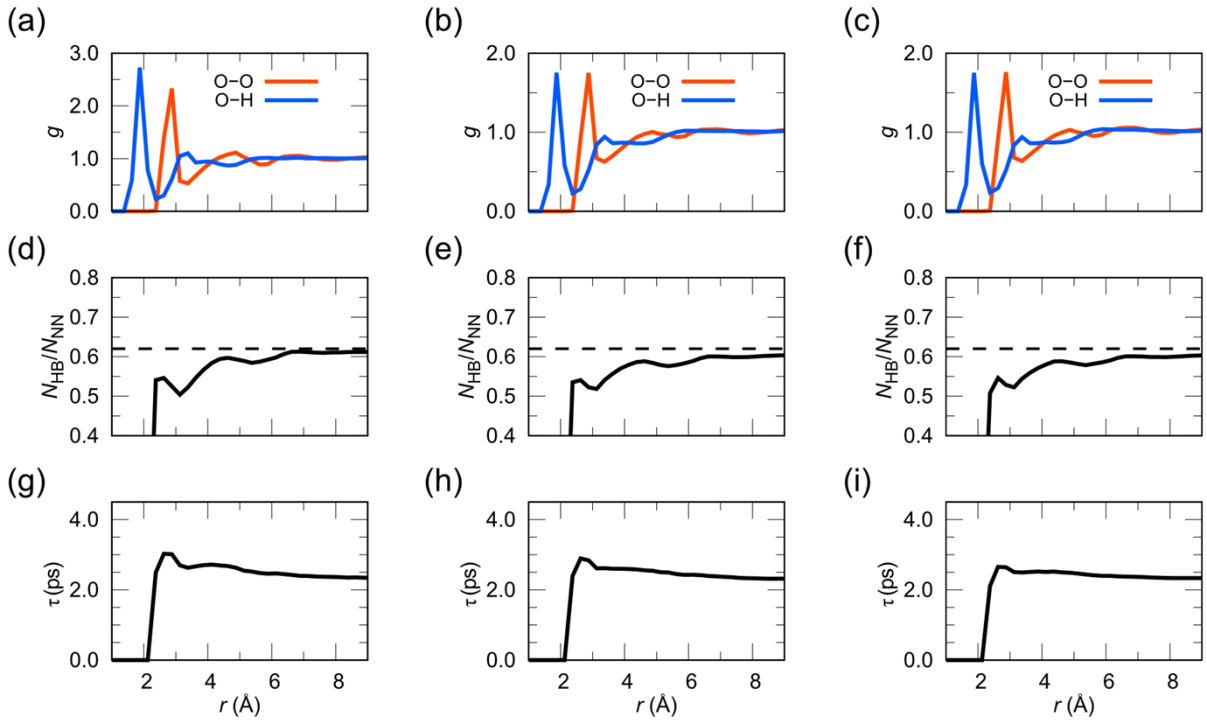

Figure S18. The radial distribution functions (RDFs, $g(r)$) of the oxygen and hydrogen atoms of water molecules around the O atoms of (a) phenylalanine, (b) L-serine acrylate, and (c) L-propionyl serine; the normalized values of N_{HB}/N_{NN} around the O atoms of (d) phenylalanine, (e) L-serine acrylate, and (f) L-propionyl serine, with the dashed line indicating the value for pure water; and the rotational relaxation time τ around O atoms of (g) phenylalanine, (h) L-serine acrylate, and (i) L-propionyl serine, where r is the interatomic distance.

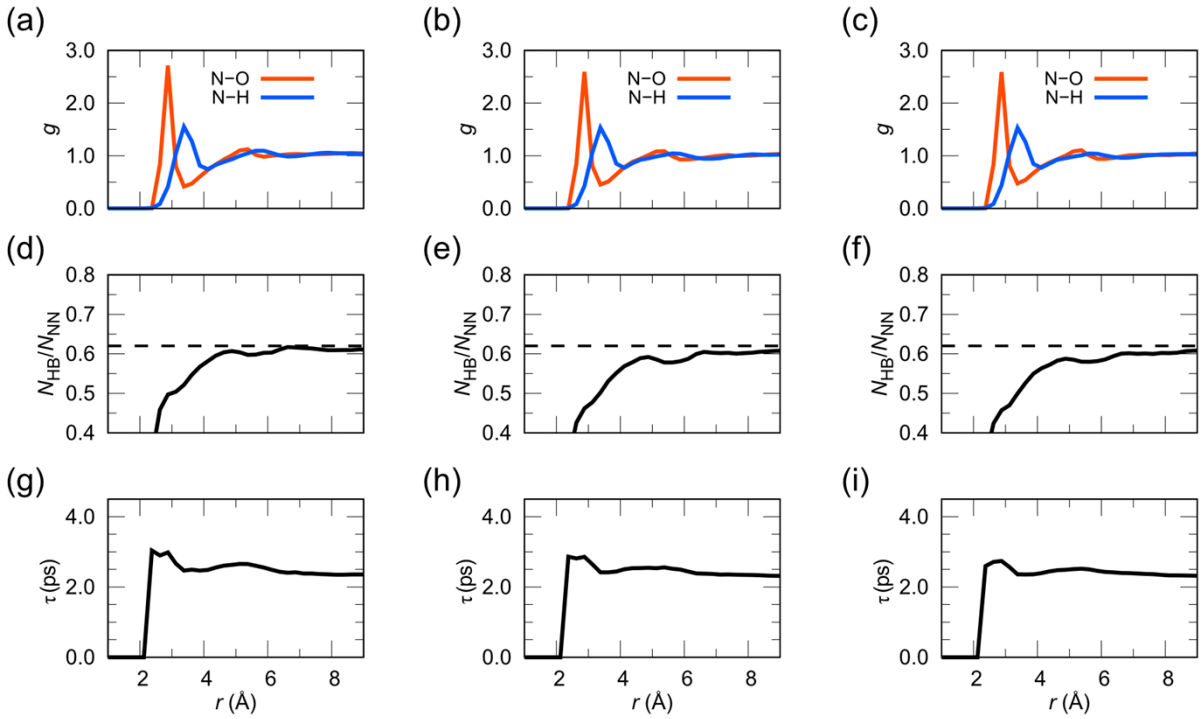

Figure S19. The radial distribution functions (RDFs, $g(r)$) of the oxygen and hydrogen atoms of water molecules around the N atoms of (a) phenylalanine, (b) L-serine acrylate, and (c) L-propionyl serine; the normalized values of N_{HB}/N_{NN} around the N atoms of (d) phenylalanine, (e) L-serine acrylate, and (f) L-propionyl serine, with the dashed line indicating the value for pure water; and the rotational relaxation time τ around N atoms of (g) phenylalanine, (h) L-serine acrylate, and (i) L-propionyl serine, where r is the interatomic distance.

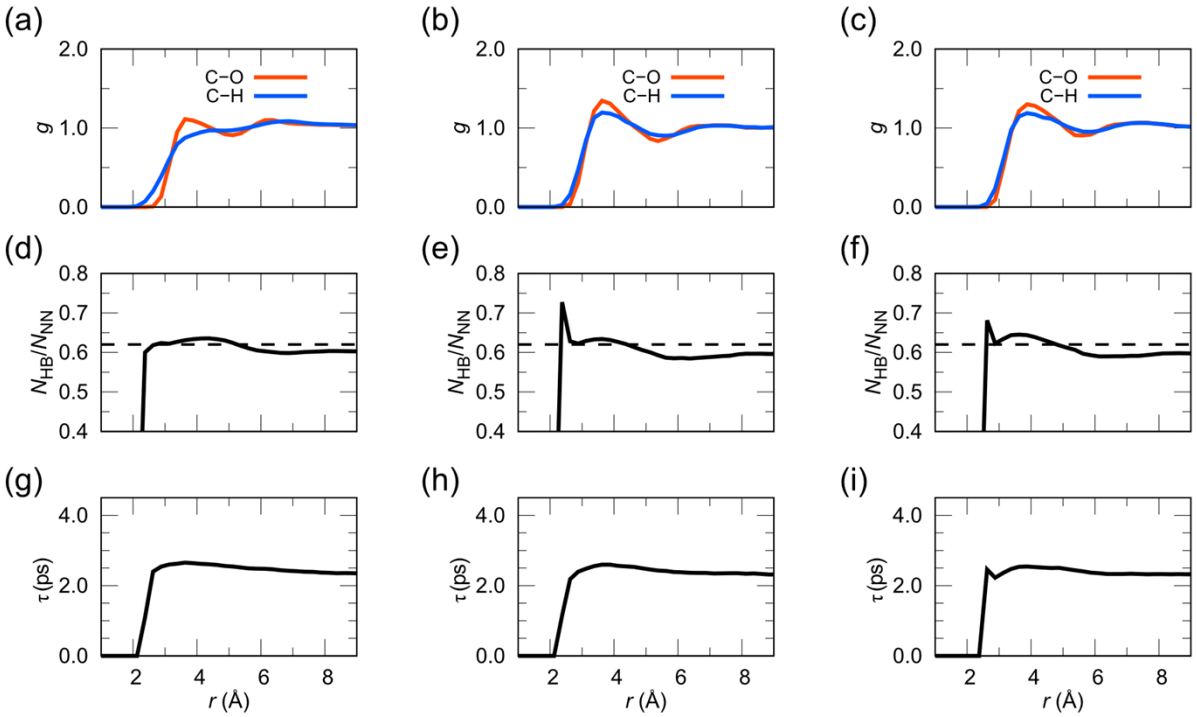

Figure S20. The radial distribution functions (RDFs, $g(r)$) of the oxygen and hydrogen atoms of water molecules around the C atoms at the end opposite the zwitterionic moiety of (a) phenylalanine, (b) L-serine acrylate, and (c) L-propionyl serine; the normalized values of N_{HB}/N_{NN} around the C atoms at the end opposite the zwitterionic part of (d) phenylalanine, (e) L-serine acrylate, and (f) L-propionyl serine, with the dashed line indicating the value for pure water; and the rotational relaxation time τ around C atoms at the end opposite the zwitterionic part of (g) phenylalanine, (h) L-serine acrylate, and (i) L-propionyl serine, where r is the interatomic distance. The number of C atoms analyzed here is 6, 2, and 2 for phenylalanine, L-serine acrylate, and L-propionyl serine, respectively.

Reference:

(1) M. Nagao, M. Kichize, Y. Hoshino and Y. Miura, *Biomacromolecules*, 2021, **22**, 3119–3127.

(2) L. Martínez, R. Andrade, E. G. Birgin and J. M. Martínez, *J. Comput. Chem.*, 2009, **30**, 2157–2164.

(3) B. Hourahine, B. Aradi, V. Blum, F. Bonafé, A. Buccheri, C. Camacho, C. Cevallos, M. Y. Deshaye, T. Dumitrică, A. Dominguez, S. Ehlert, M. Elstner, T. van der Heide, J. Hermann, S. Irle, J. J. Kranz, C. Köhler, T. Kowalczyk, T. Kubař, I. S. Lee, V. Lutsker, R. J. Maurer, S. K. Min, I. Mitchell, C. Negre, T. A. Niehaus, A. M. N. Niklasson, A. J. Page, A. Pecchia, G. Penazzi, M. P. Persson, J. Řezáč, C. G. Sánchez, M. Sternberg, M. Stöhr, F. Stuckenberg, A. Tkatchenko, V. W.-z. Yu and T. Frauenheim, *J. Chem. Phys.*, 2020, **152**, 124101.

(4) M. Gaus, A. Goez and M. Elstner, *J. Chem. Theory Comput.*, 2013, 9, 338−354.

(5) M. Kubillus, T. Kubar, M. Gaus, J. Řezác, and M. Elstner, *J. Chem. Theory Comput.*, 2015, **11**, 332−342.

(6) P. Goyal, H.-J. Qian, S. Irle, X. Lu, D. Roston, T. Mori, M. Elstner and Q. Cui, *J. Phys. Chem. B*, 2014, **118**, 11007−11027.

(7) J. Řezác, *J. Chem. Theory Comput.,* 2017, **13**, 4804−4817.

(8) T. H. Choi, R. Liang, C. M. Maupin, G. A. Voth, *J. Phys. Chem. B*, 2013, **117,** 5165−5179.

(9) A. W. Sakti, Y. Nishimura and H. Nakai, *J. Phys. Chem. B*, 2017, **121**, 1362−1371.

(10) Y. Higuchi, Y. Asano, T. Kuwahara and M. Hishida, *Langmuir*, 2021, **37**, 5329−5338.

(11) J. L. F. Abascal and C. Vega, *J. Chem. Phys.*, 2005, **123**, 234505.

(12) G. J. Martyna, M. E. Tuckerman, D. J. Tobias and M. L. Klein, *Mol. Phys*., 1996, **87**, 1117−1157.

(13) H. J. C. Berendsen, J. P. M. Postma, W. F. van Gunsteren, A. DiNola, J. R. Haak, *J. Chem. Phys.*, 1984, **81**, 3684−3690.

(14) E. Pluharǒ vá, P. Jungwirth, N. Matubayasi and O. Marsalek, *J. Chem. Theory Comput.*, 2019, **15**, 803−812.

(15) J. Martí, J. A. Padro and E. Guàrdia, *J. Chem. Phys.*, 1996, **105**, 639−649.